2023 년 2 월

석사학위 논문

Effect of *Castanopsis sieboldii* extract on UVB-induced skin aging

조선대학교 대학원

약 학 과

이 혜 림

Effect of *Castanopsis sieboldii* extract on UVB-induced skin aging

구실잣밤 잎 추출물의 피부 노화 억제 효능 연구

2023 년 2 월 24 일

조선대학교 대학원

약 학 과

이 혜 림

Effect of *Castanopsis sieboldii* extract on UVB-induced skin aging

지도교수 기 성 환

이 논문을 약학 석사학위신청 논문으로 제출함

2022년 10월

조선대학교 대학원

약 학 과

이 혜 림

이혜림의 석사학위논문을 인준함

위원장 조선대학교 교수 최 홍 석 인

위 원 조선대학교 교수 이 금 화 인

위 원 조선대학교 교수 기 성 환 인

2022 년 12 월

조선대학교 대학원

CONTENTS

LIST OF FIGURES

ABBREVIATIONS

UVB	ultraviolet B
ER	endoplasmic reticulum
CS	*Castanopsis sieboldii*
CSL	*Castanopsis sieboldii* leaf
CSL3	70% EtOH extract of *Castanopsis sieboldii* leaf
EGCG	epigallocatechin gallate
t-BHP	tert-butyl hydroperoxide
ECM	extracellular matrix
MMP	matrix metalloproteinase
AP-1	activator protein 1
MAPKs	Mitogen-activated protein kinases
UPR	unfolded protein response
TPC	Total polyphenol content
TFC	Total flavonoid content
MTT	3-(4,5-dimethyl-2-thiazolyl)-2,5-diphenyl-2H-tetrazolium bromide
DCFH-DA	2′,7′-dichlorofluorescein diacetate
PBS	phosphate buffered saline
mTOR	mammalian target of rapamycin
EtOH	ethanol

국 문 초 록

구실잣밤 잎 추출물의 피부 노화 억제 효능 연구

이 혜 림

지 도 교 수: 기 성 환

약학과

조선대학교 대학원

피부는 인체에서 가장 큰 기관이며, 체온조절, 수분손실 억제, 물리적 손상으로부터 방어 기능을 한다. 피부는 표피, 진피, 피하조직 3 개의 층으로 나뉘어져 있고 그 중 표피는 가장 바깥쪽에 위치하며 자외선(Ultra violet, UV), 미세먼지, 중금속, 병원성 미생물 등에 가장 많이 노출되고 손상을 받는 부위이다. 그 중 자외선은 자연환경에서 쉽게 피부에 직접적으로 노출된다. 자외선 (UV)는 파장에 따라 UVA (315−400 nm), UVB (280−315 nm), UVC (100−280 nm)로 나뉘게 된다. UVC 는 오존층에 의해 흡수되고 피부에 도달하는 자외선 중 UVB 는 급성 노출 시 표피에 심한 손상을 야기한다. UVB 는 표피에서 활성산소종 (ROS)을 증가시키고 산화적 스트레스를 유발한다. UVB 에 의해 증가된 산화적 스트레스는 소포체 등의 세포 소기관을 손상시키며, 궁극적으로 세포사멸을 일으키게 된다. 또한 ROS

는 콜라겐을 분해하는 MMP(Matrix Metalloproteinase)의 발현을 증가시켜 콜라겐을 분해하고 프로콜라겐을 분해하여 피부의 광독성을 유발한다. 구실잣밤(Castanopsis sieboldii)은 아열대 동부 아시아에 자생하는 상록수 종이다. 최근 구실잣밤 나무 열매 추출물이 세포 내 ROS 를 감소시켜 산화적스트레스를 억제한다는 연구가 보고된 바 있다. 하지만 UVB 에 의한 피부 손상 및 노화에 대한 구실잣밤 잎 추출물 (CSL3)의 효능연구는 전무한 실정이다.

본 연구에서는 HaCaT 세포(Human Keratinocyte Cell Line)를 이용하여 CSL3 의 광독성 보호 효능 및 관련기전을 조사했다. UVB 와 t-BHP 는 HaCaT 세포에서 ROS 생성을 증가시켰으며 CSL3 은 이를 유의적으로 억제하였다. 또한 CSL3 은 UVB 로 인해 증가된 apoptosis 를 억제함으로 세포 생존율을 개선시켰으며 ER stress 를 농도 의존적으로 억제하였다. 나아가 CSL3 에 의해 감소되었던 ER stress 마커가 autophagy inhibitor 인 3-MA 를 처리하였을 때 다시 회복됨을 통해 CSL3 의 ER stress 억제 효능은 autophagy 를 매개함을 확인할 수 있었으며 CSL3 에 의한 autophagy 활성화는 LC3B 의 상위 인자인 mTOR 억제를 매개하였다. 우리는 마지막으로 UVB 를 조사한 HaCaT 세포에서 CSL3 의 항노화 효과를 평가하였다. UVB 에 의해 증가된 MMP 의 발현 및 감소된 콜라겐의 합성 감소가 CSL3 처치에 의해 반전되었다. 마지막으로 우리는 CSL3 의 조성 및 활성성분을 분석하였고 다량의 epigallocatechin gallate (EGCG)가 검출되었다. 예상한 대로 EGCG 는 CSL3 처리와 동일하게 autophagy 활성화, ER stress 억제를 통해 HaCaT 세포를 보호하였으며, MMP 발현과 콜라겐의 발현을 억제시켰다. 이러한 결과를 통해 CSL3 의 보호효과능 EGCG 를 매개함을 확인하였다. 결론적으로, CSL3 은 ER stress 억제 및 autophagy 활성화를 통하여 UVB 로 인한 피부 손상을 억제할 수 있는 후보물질이 될 수 있음을 제시한다.

I. INTRODUCTION

Skin is the largest organ in the body, and divided into three layers (epidermis, dermis, and subcutaneous tissue). Among them, the epidermis is the outermost and is the most exposed and damaged area to ultraviolet (UV) rays, fine dust, and pathogenic microorganisms. UV is most easily exposed to the skin and is organized of UVA (315-400 nm), UVB (280-315 nm), UVC (100-280 nm) [1]. UVC is consumed by ozone layer but UVA and UVB get at skin. Especially, UVB has a stronger wavelength than UVA and causes more damage to skin. It is widely known that UVB produces ROS [2]. These ROS cause various skin damage such as inflammation, aging and skin cancer [3]. In addition, ROS ultimately induces programmed cell death like to apoptosis and autophagy, or unprogrammed cell death such as a necrosis [4]. Therefore, excavating anti-oxidants materials is very important for suppressing skin damage.

Skin aging is caused by photodamage by UVB irradiation. The feature of skin aging is decomposition of extracellular matrix (ECM) [5]. The ECM acts like cell adhesion, cell-to-cell communication and differentiation in skin. UVB decomposes ECM such as collagen and elastin by inducing matrix metalloproteinase (MMP) expression [6]. Especially, MMP -3, -9 act as major collagenase [7]. MMP expression is transcriptionally controled by activator protein 1 (AP-1) and is upregulated by UVB-inducing c-Jun or c-Fos [8]. Therefore, up-regulation of MMP by UVB maybe cause of skin aging. Keratinocytes are the major cell type of the epidermis where they prossess more than 90% of the overall skin cells [9; 10]. Also, keratinocyte protects the skin from external factors that induce aging [11]. However, UVB induces photodamage and skin aging by activating MMP in keratinocyte [12].

Endoplasmic reticulum (ER) stress was generated by misfolded and unfolded protein called unfolded protein response (UPR) [13]. When these phenomena occur repeatedly, cell death eventually occurs [14]. Therefore, it is important to remove the damaged ER to keep cellular homeostasis. Autophagy is known to be an essential lysosome-dependent cell survival

mechanism through the elimination and recycling of UPR and intracellular components damaged by various stimulations [15]. Especially, mammalian target of rapamycin (mTOR), a serine/threonine kinase, is a regulator of cellular metabolism and a sensor of cellular nutritional status [16]. mTOR pathway performs an essential role in autophagy regulation and inhibition of mTOR potently induces autophagy [17]. Recently, it has been reported that activation of mTOR increased damaged ER and mitochondria [18]. Hence, inhibition of mTOR might be an effective strategy for reducing ER stress. Mitogen-activated protein kinases (MAPKs) are major upstream modulators of mTOR and have been reported to have capability to reduce ER stress [19].

Castanopsis sieboldii (CS) is species of evergreen tree that lives in subtropical eastern Asia. It is known to have antioxidant activity and reduces oxidative stress by decreasing intracellular ROS [20]. Also, CS inhibited inflammatory response in macrophages by LPS stimulation [21]. Although CS has been known to perform several pharmacological actions like to anti-oxidative and anti-inflammatory influences, pharmacological efficacy of CS on photodamage and skin aging in UVB-irradiated keratinocytes had never been examined yet.

In this study, we thus explored cytoprotective effect of 70% EtOH efficacy of *C. sieboldii* leaf (CSL) in HaCaT cells (human keratinocyte cell line) irradiated with UVB. Our data suggests that UVB increased ROS generation and cytotoxicity which were attenuated by 70% ethanol (EtOH) extract of CSL (CSL3) treatment via autophagy-dependent ER stress inhibition. Furthermore, quantitative analysis of CSL3 were analyzed by HPLC-MS and composition of the polyphenols was also discussed. Therefore, CSL3 may be applied as a promising efficient material for anti-skin aging productions, which can control skin damage and the decomposition of ECM proteins including collagen by MMPs.

II. MATERIALS AND METHODS

1. Materials

Anti-LC3B antibody was gained by NOVUS Biologicals (Littleton, CO, USA). Anti-p62 antibody was get from Abnova (Taipei, Taiwan). Anti-GRP78 antibody was gained from Abcam (Cambridge, MA, USA). Anti-CHOP, ERK, JNK, p38, phospho-ERK, phospho-JNK, phospho-p38, phospho-mTOR, mTOR, Caspase-3, phospho-Akt antibodies were provided from Cell signaling Technology (Danvers, MA, USA). Bax and PARP antibodies were obtained from Santa Cruz Biotechnology (Santa Cruz, CA, USA). Horseradish peroxidase-conjugated goat anti-mouse and anti-rabbit antibodies were gained from Invitrogen (Carlsbad, CA, USA). 3-(4,5-dimethyl-2-thiazolyl)-2,5-diphenyl-2H-tetrazolium bromide (MTT), 2′,7′-dichlorofluorescein diacetate (DCFH-DA), tert-butyl hydroperoxide (t-BHP), epigallocatechin-gallate (EGCG), 2,2-diphenyl-1-picrylhydrazyl (DPPH), (2,2'-azino-bis(3-ethylbenzothiazoline-6-sulfonic acid) diammonium salt) (ABTS), ethanol (EtOH), methanol, Sodium carbonate, aluminum chloride ($AlCl_3$), Folin-Ciocalteu (F-C)'s phenol reagent acetic acid, gallic acid, epicatechin, rutin, tannic acid, naringin, quercetin and β-actin antibody were acquired from Sigma Aldrich (St. Louis, MO, USA).

2. Chemical extracts of CSL

CS were collected in Wando-gun, Jeollanam-do, Korea, during the summer season of 2020. The fresh CSL were dried at 40 °C. The dried leaves (10 g) were powdered and extracted with several methods described in Figure 1A. Powdered CSL were abstracted with water at 1.0 atm and 100 °C for 1 h (autoclaving). CSL powder were extracted with water using ultrasonic (POWER SONIC 520, Hwashin Tech Co., Ltd, Seoul, Korea), and 25 °C for 4 h. Diverse density of EtOH (70%, and 100%) were employed to abstract CSL for 7 days at room temperature (25 ± 2 °C). The four extracts were vacuum-concentrated. The final each solvent

and method were named as autoclaving (CSL1), ultrasonic (CSL2), 70% EtOH (CSL3), 100% EtOH (CSL4).

3. DPPH radical scavenging activity

DPPH radical scavenging activity was measured by modified manner of Blois [22]. 200 μL of each concentration sample and 800 μL of 0.5 mM DPPH reagent were mixed and vortexed, followed by reaction in the dark for 15 minutes. Absorbance was estimated at 517 nm wavelength using a Synergy HT multi-detection microplate reader (Biotek, VT, USA). Each sample was performed three times to obtain an average value, and ascorbic acid was employed as a positive control. The radical scavenging activity of each solution was measured by the following equation and expressed as a percentage: Radical scavenging activity (%) = ($Abs_{control}$ – Abs_{sample}) / $Abs_{control}$ × 100, where $Abs_{control}$ is the absorbance of the MeOH control, and Abs_{sample} is the absorbance in the presence of the CSL extracts.

4. ABTS radical scavenging activity

ABTS radical scavenging activity was measured by modified of Re et al. [23]. 7 mM ABTS was mixed with 2.45 mM potassium persulfate in the same volume and reacted in the dark for 18 h to form ABTS radical. The ABTS radical solution was diluted with distilled water and the absorbance value at 730 nm was adjusted to 0.90 ± 0.02. 200 μL of each concentration sample and 1000 μL of ABTS radical solution were mixed and vortexed, followed by reaction in the dark for 15 min. Absorbance was evaluated at 730 nm wavelength using a Synergy HT multi-detection microplate reader (Biotek, VT, USA). The radical scavenging activity of each solution was measured by the following equation and expressed as a percentage: Radical scavenging activity (%) = ($Abs_{control}$ – Abs_{sample}) / $Abs_{control}$ × 100, where $Abs_{control}$ is the absorbance of the MeOH control, and Abs_{sample} is the absorbance in the presence of the CSL extracts.

5. Total phenol and flavonoid contents

Total polyphenol content (TPC) was evaluated using the modified Folin-Ciocalteu method [24]. 500 μL of 1 mg/mL CSL extracts, 500 μL of 0.2 M Folin-Ciocalteu's phenol reagent and 500 μL of 2% sodium carbonate were mixed and vortexed, followed by reaction in the dark for 30 min. Absorbance was evaluated at 750 nm wavelength using a Synergy HT multi-detection microplate reader (Biotek, VT, USA). TPC was represented as mg/g of gallic acid equivalent (GAE) based on the calibration curve using the following equation: $y = 8.4755x + 0.1105$, $R^2 = 0.9779$, where x was the absorbance and y was the GAE (mg/g).

Total flavonoid content (TFC) was measured using the modified Kim et al. method [25]. 500 μL of 1 mg/mL CSL extracts, 100 μL of 10% aluminum chloride, 100 μL of 1 M potassium acetate, 1.5 mL of methanol and 2.8 mL of distilled water were mixed and vortexed, followed by reaction in the dark for 40 min. Absorbance was evaluated at 415 nm wavelength using a Synergy HT multi-detection microplate reader (Biotek, VT, USA). TFC was expressed as mg/g of quercetin equivalent based on the calibration curve using the following equation: $y = 3.1736x + 0.0397$, $R^2 = 0.9998$, where x was the absorbance and y was the quercetin equivalent (mg/g).

6. High-Performance Liquid Chromatography with Diode-Array Detection (HPLC–DAD) Analysis

The extracts of CSL (CSL1-CSL4) were analyzed quantitatively by HPLC-DAD (SPD-20A, SHIMADZU CO., Japan). Seven standards (gallic acid, epicatechin, EGCG, rutin, tannic acid, naringin, quercetin) were selected for the experiment, and HPLC analysis conditions were as follows. The column is Shimpack GIS-ODS (C18, 4.6×250 mm, 5.0 μm, Shimadzu Co., Japan). The flow rate is 0.7 mL/min. The temperature is 30℃. The injection volume is 20 μL. The UV detector wavelength is 280 nm. As the mobile phase, 0.1% acetic acid in water (solvent A) and 0.1% acetic acid in methanol (solvent B) were used. The gradient conditions of the mobile phase are 0 min: B (10%), 0-5 min: B (10%), 5-15 min: B (40%), 15-45 min: B (60%), 45-55 min: B

(80%), 55-60 min: B (100%), 60-65 min: B (10%), 65-70 min: B (10%). The injection volume was 20 μL. All samples used for analysis were filtered with a 0.45 μm filter.

7. Cell culture

HaCaT cells (Human Keratinocyte Cell Line) were cultivated in 60 mm (Thermo Scientific, Waltham, MA, USA) plates, and raised to 70-80% confluency. HaCaT Cells were cultivated Dulbecco's modified Eagle medium with 10% fetal bovine serum (Atlas Biologicals, Fort Collins, CO, USA), 1% penicillin/streptomycin at 37℃ in a humidified 5% CO_2 atmosphere.

8. MTT assay

To investigate cytotoxicity of CSL3, HaCaT cells were cultivated a concentration of 1×10^5 cells/well in 24 well plates and processed with various concentration of CSL3 for 12h. Then, to identify the cytoprotective effect of CSL3 on photodamaged HaCaT cells, the cells were pretreated CSL3 (30 or 100 μg/mL) for 1 h and incubated with UVB (30 mJ/cm^2) or *t*-BHP (600 μM) for 6 h. After treat, the cells were treated with MTT (0.2 mg/mL) for 30 min to verify viable cells. Formazan crystals generated in the plates were dissolving by adding 300 μL of dimethyl sulfoxide. The absorbance was measured at 550 nm using a microplate reader (Spectra MAX, Molecular Device, Sunnyvale, CA, USA).

9. UVB irradiation

HaCaT cells cultivated at 4×10^5 cells/well in 60 mm plate. After 24 h, the culture medium was changed with a serum-free medium and cultivated for 3 h. Then, cells were processed with CSL3 (30 or 100 μg/mL) for 1 h. To irradiate UV, the cells were rinsed with phosphate buffered saline (PBS) and added with 1 mL PBS. BIO-LINK BLX UV lamp (wavelength 312 nm, BIO-LINK BLX) was employed for UVB radiation and the radiation was conducted at 15

cm distance for 30 mJ/cm$^{2.}$

10. Immunoblot analysis

Protein extraction, SDS polyacrylamide gel electrophoresis, and immunoblot analysis were processed as formerly reported [26]. Simply, cell lysates were divided by SDS-PAGE (6%, 7.5%, 12% acrylamide gels) and electrophoretically being transferred to a nitrocellulose (NC) membrane (GE Healthcare, IL, USA). Subsequently, the NC membranes were blocked with 5% skim milk at 37℃ and incubated overnight at 4℃ with the primary antibody. After eliminating primary antibody, NC membranes were rinsed with PBS three times for 10 minutes. The NC membranes were cultivated with a secondary antibody (Invitrogen, Carlsbad, CA, USA) for 1 h at room temperature. After washing, NC membranes were treated with enhanced chemiluminescence detection kit (Amersham Biosciences, Buckinghamshire, UK). Immunoreactive protein expression was visualized using LAS 4000 (Fujifilm, Tokyo, Japan). β-actin was used as immunoblotting control.

11. RNA isolation and RT-PCR analysis

TRIzol (Invitrogen, Waltham, MA, USA) was used to obtain total RNA extract abide by the manufacturer's protocol. To synthesis cDNA, total RNA (2 μg) was reverse-transcribed using oligo dT_{18} primer. The cDNA synthesized was amplified using a high-capacity cDNA synthesis kit (Bioneer, Daejeon, Korea) with a thermal cycler (Bio-Rad, Hercules, CA, USA). PCR intensified samples were divided by using 2% agarose gel, included ethidium bromide (Sigma, St. Louis, MO, USA), and imaged in gel documentation system (Fujifilm, Tokyo, Japan). The following primer sequences were used: human MMP-2 sense 5′-ACAGCAGGTCTCAGCCTCAT -3′, and antisense 5′-TGAAGCCAAGCGGTCTAAGT -3′; human MMP-3 sense 5′-AACCTGTCCCTCCAGAACCT-3′, and antisense 5′-GGAAGAGATGGCCAAAATGA-3′; human MMP-9 sense 5′-

CTCGAACTTTGACAGCGACA-3′, and antisense 5′-GCCATTCACGTCGTCCTTAT-3′; human Col1A1 sense 5′-CACAGAGGTTTCAGTGGTTTGG -3′, and antisense 5′-GCACCAGTAGCACCATCATTTC -3′; human GADD153/CHOP sense 5′-AGGGAGAACCAGGAAACGGAAACA -3′, and antisense 5′-TCCTGCTTGAGCCGTTCATTCTCT -3′; human GRP78/Bip sense 5′-GAGATCATCGCCAACGATCAG -3′, and antisense 5′-ACTTGATGTCCTGCTGCACAG -3′;human GAPDH sense 5′-GAAGGTGAAGGTCGGAGTC-3′, and antisense 5′-GAAGATGGTGATGGGATTTC-3′. GAPDH was used as a reference gene for normalization.

12. Measurement of ROS production

DCFH-DA fluorescent probe was untilized to measure productions of intracellular ROS. Pretreated with CSL3 (30 or 100 μg/mL) for 1 h and irradiated with UVB (30 mJ/cm^2). After treatment, HaCaT Cells were splotched with 10 μM DCFH-DA for 30 min at 37℃ in the dark. Next, the cells were rinsed with PBS and were scraped. Productions of intracellular ROS was observed under fluorescence microplate reader (Gemini, Molecular Devices, Sunnyvale, CA, USA) at excitation/ emission wavelengths of 485 nm/530 nm.

13. Cell apoptosis Assay

The cell apoptosis level was investigated by using a FITC Annexin V Apoptosis Detection kit (BD Biosciences, NJ, USA) abide by the manufacturer's protocols and as previously described [27]. Simply, HaCaT cells cultured at 4 × 10^5 cells/well in 6 well plate. Cells were changed serum-free medium for 3 h and treated CSL3 (30 μg/mL) for 1 h. After treat, cells were processed with UVB (30 mJ/cm^2) then incubated for 3 h. Subsequently, the cells were rinsed with PBS three times and harvested by trypsin and centrifuged (4℃, 3000g, 3 min). Pellets were resuspended 1X Annexin V binding buffer. The pellets were treated with 1% Propidium Iodide Staining Solution and 1% FITC Annexin V for 20 min in the dark. Apoptotic cells were

investigated using Flow-cytometry (Beckman-Coulter, Brea, CA, USA).

14. Procollagen Type I measurement

The synthesized procollagen levels in culture media were assessed by using Procollagen Type I C-peptide EIA Kit (Takara Biochemical Inc., Japan) abide by the manufacturer's instruction. Briefly, the cells cultivated at 4×10^5 cells/well in 60 mm plate. Cells were treated with UVB (30 mJ/cm^2) in the presence or absence of CSL3 (30 or 100 μg/mL). After treatment, the culture media was obtained in the plate. Antibody-POD conjugate solution and sample were added in antibody coated microtiterplate and cultivated at 37℃ for 3 h. Subsequently, the cells were rinsed PBS four times and added substrate solution for 15 min. The absorbance was evaluated at 450 nm using a microplate reader (Spectra MAX, Molecular Device) after adding stop solution.

15. Wound healing assay

Culture-Inserts Kit (Ibidi, Gräfelfing, Germany) were used to evaluate cell migration. HaCaT cells cultivated at 5×10^5 cells/well in culture inserts. The cells were treated with UVB (30 mJ/cm^2) in the presence or absence of CSL3 (30 or 100 μg/mL). Then removed culture insert. After 12 h, The scratched area was visualized microscope (Axiovert 200 M, Carl ZEISS, Germany).

16. Statistical analysis

One-way ANOVA was used to assess significant differences between treatment groups. The Newman-Keuls test was used to assess the significance of the differences between the means of multiple groups. Results are expressed as mean ± standard error (SE).

III. RESULTS

1. CSL3 has high anti-oxidative efficacy compared to others CSL extracts

CSL were extracted using water, ultrasonic and ethanol (70% - 100% EtOH). The antioxidant efficacies of CSL extracts were measured for radical scavenging activities using DPPH, ABTS (Fig 1B). Ascorbic acid was used as a positive control. The concentrations of the extracts were from 10 to 500 μg/mL and the IC_{50} of the 70% EtOH extract of CSL (CSL3) was 22.24 ± 1.96 μg/mL in the DPPH assay, 60.20 ± 2.37 μg/mL in the ABTS assay. CSL3 had the largest antioxidant activity among all extracts in all radical scavenging activity. Ascorbic acid, used as the positive control, showed an IC_{50} of 36.61 ± 1.92 μg/mL in the DPPH assay and 37.37 ± 2.11 μg/mL in the ABTS assay.

In the previous study, the IC_{50} value of the 80% ethanol extract of CSL was 16.26 μg/mL, which was confirmed as a result similar to that of this study [20]. Youn et al. (2017) measured the antioxidant activities of a methanol extract of the fruits' bark of *Castanopsis sieboldii* at a concentration of 50 μg/mL [28]. DPPH and ABTS activities were 75% and 98%, respectively, and had very high antioxidant activities at low concentrations. In conclusion, the CSL3 contain high anti-oxidative efficacy compared to others CSL extracts.

A)

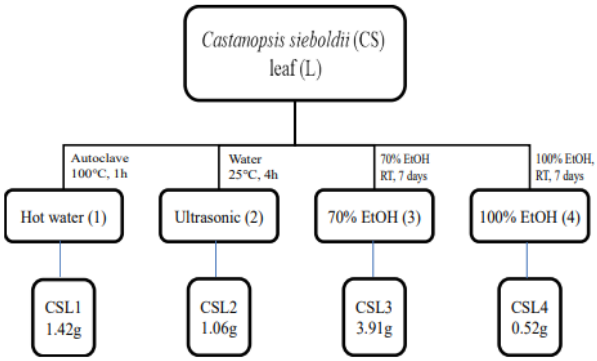

B)

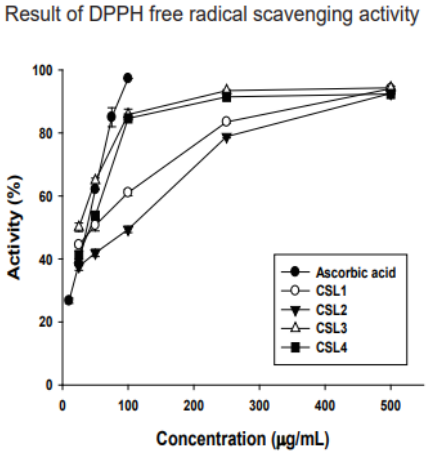

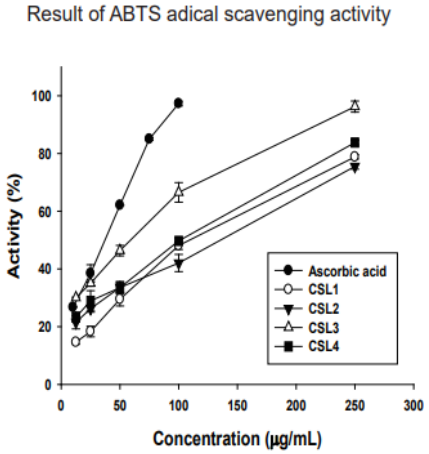

Sample	DPPH IC_{50} (μg/mL)	ABTS IC_{50} (μg/mL)	TPC (GAE mg/g)	TFC (QUE mg/g)
CSL1	47.40 ± 2.00	104.58 ± 3.66	133.50 ± 0.41	15.08 ± 0.19
CSL2	95.63 ± 3.32	133.74 ± 4.12	131.97 ± 0.43	13.94 ± 0.39
CSL3	22.24 ± 1.96	60.20 ± 2.37	152.81 ± 7.35	31.72 ± 0.63
CSL4	41.34 ± 2.37	111.89 ± 4.20	108.88 ± 2.73	22.46 ± 2.55
Ascorbic acid	36.61 ± 1.92	37.37 ± 2.11	-	-

Figure 1. Extraction method and anti-oxidative efficacy measurement of CSL extracts

(A) Schematic diagram of extraction methods of *Castanopsis sieboldii* leaves. (B) Antioxidant activity results: 2,2-diphenyl-1-picrylhydrazyl (DPPH) and 2,2-azino-bis (3-ethylbenzthiazoline-6-sulfonic acid) (ABTS).

2. CSL3 protects HaCaT cells by reducing apoptosis

To identify cytotoxicity of CSL3 in keratinocytes, we assessed cell viability in various concentration (25, 50, 100 μg/mL) using HaCaT cells. Results suggested that up to 100 μg/mL of CSL3 were not considerably different from that of the vehicle-treated group (Fig 2A). Next, we assessed anti-oxidative effect of CSL3 by using DCFH-DA. CSL3 prominently prohibited the increased ROS generation by UVB irradiation (30 mJ/cm^2) (Fig 2B). Also, treatment with CSL3 antagonized ROS production by *t*-BHP (Fig 2C). Therefore, we identified that CSL3 diminish oxidative stress by ROS. After, we evaluated cytoprotective effect against UVB by using MTT assay. We discovered that CSL3 improved decreased cell viability by UVB treatment in a concentration-dependent manner (Fig 2D). Under the microscopy, CSL3 definitely improved damaged HaCaT cells by UVB (Fig 2E). It was well established that UVB led to apoptosis [29]. We thus evaluated whether CSL3 could inhibit apoptosis by UVB irradiation. The increased cleaved Caspase-3 due to UVB was effectively diminished by CSL3 pretreatment. Apoptosis regulator Bax and PARP were also decreased by CSL3 treatment (Fig 2F). In addition, apoptosis level was investigated by Annexin V/PI staining. The result showed that treatment of CSL3 reduces increased apoptosis by UVB irradiation (Fig 2G). Consequently, these results suggested that the anti-oxidant capacity of CSL3 protects UVB-damaged HaCaT cells via apoptosis inhibition.

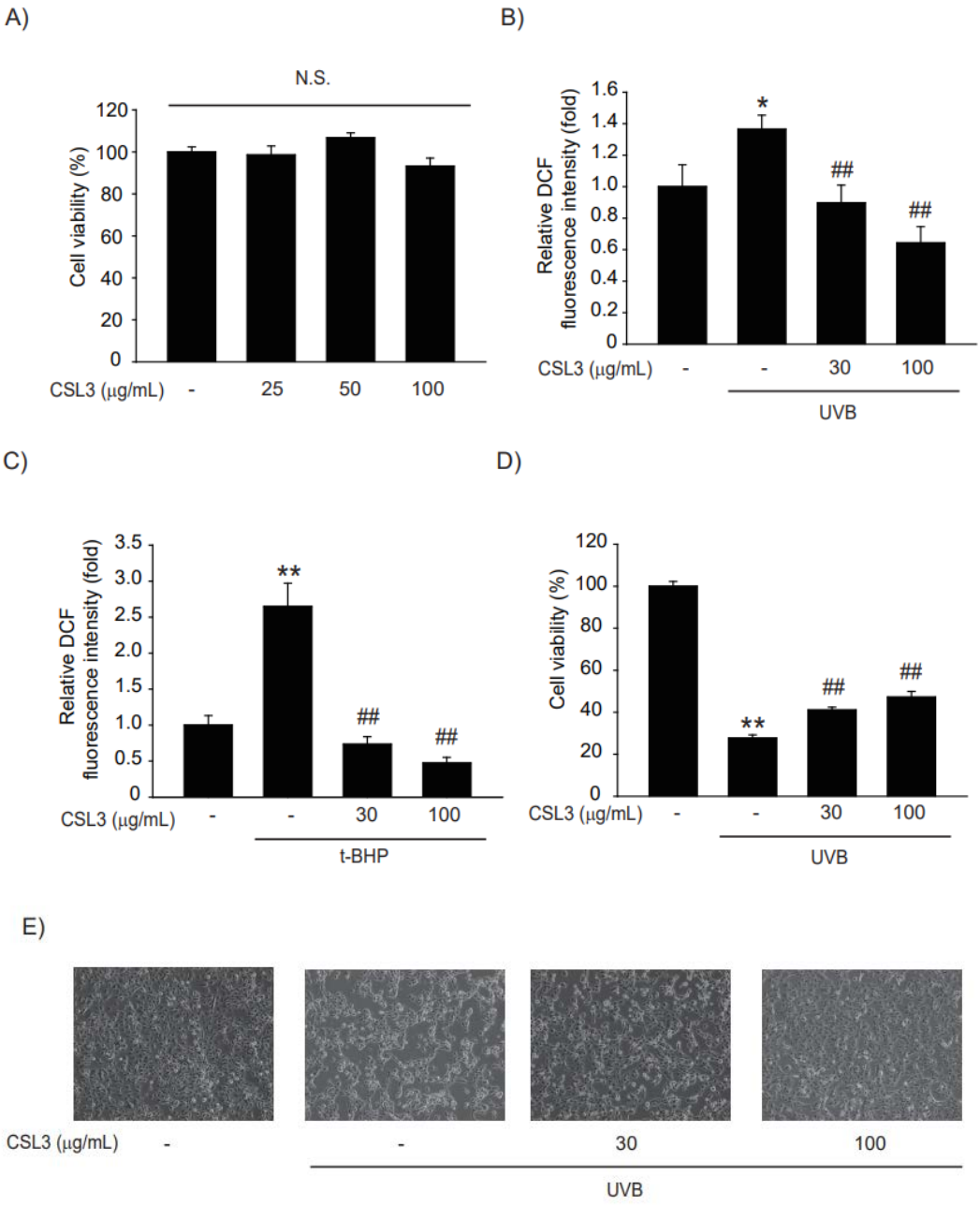

F)

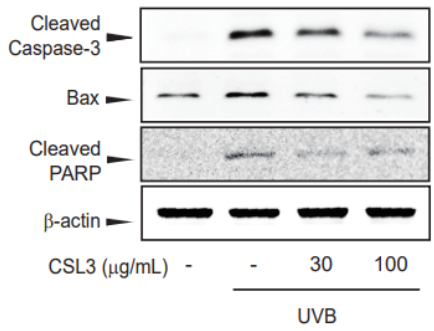

G)

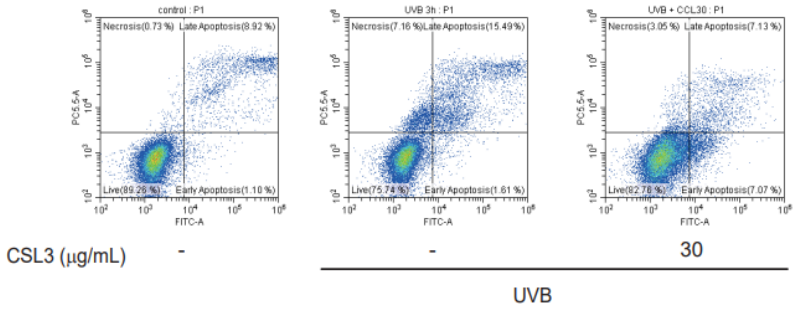

Figure 2. Effects of CSL3 on the viability of HaCaT cells

(A) The cytotoxic effect of *Castanopsis sieboldii* leaves (CSL3) in the HaCaT was decided at diversity of concentrations for 12 h by MTT assay. (B, C) The effectiveness of CSL3 on the intercellular ROS production by UVB (30 mJ/cm^2) or *t*-BHP treatment (600 μM) in HaCaT cells. The cells were processed with UVB or *t*-BHP with or without CSL3. The level of ROS formation was assessed after UVB or *t*-BHP treatment for 1 h. (n = 3, significant when compared with respective controls, * $p<0.05$, **$p<0.01$, compared with the UVB or *t*-BHP treatment group, ## $p<0.01$) (D) The cytoprotective effect of CSL3 on photodamaged HaCaT cells. The cells were treated with UVB for in the presence or absence of CSL3 for 6 h, and assessed cell viability via MTT assay. (n = 3, significant when compared with controls, * $p<0.05$, **$p<0.01$, compared with the UVB or *t*-BHP treatment group, ## $p<0.01$) (E) Microscope analysis. HaCaT cells were processed with CSL3 for 1 h. Cells were then treated with UVB for 3 h and cell morphology was visualized by microscope (Axiovert 200 M, Carl ZEISS, Germany). (F) The effect of CSL3 on apoptosis. Proteins associated with apoptosis were examined by immunoblotting. (G) Flow cytometry analysis for apoptosis. Apoptosis level was surveyed by flow cytometry. HaCaT cells were incubated with CSL3 (30 μg/mL) for 1 h. Cells were then irradiated with UVB (30 mJ/cm^2) for 3 h.

3. CSL3 inhibits ER stress by UVB irradiation

ER stress damaged cell organelles and UVB is well known as ER stress inducer [30]. Next, we investigated protective capacity of CSL3 on ER stress induced by UVB. Immunoblotting data showed that CHOP and GRP78, representative markers of ER stress, were increased by UVB irradiation and but CSL3 prohibited its expression (Fig 3A). RT-PCR analysis confirmed CSL3 effect on UV-mediated ER stress (Fig 3B). It was well reported that autophagy induction can repair damaged cell organelles induced by a diversity of insult [31]. UVB irradiation inhibited autophagy as evidenced by LC3B-II, which were reversed by treatment with CSL3. Rapamycin was used as a positive control (Fig 3C). 3-Methyladenine, an autophagy inhibitor, antagonized inhibition of UVB-mediated CHOP expression by CSL3 (Fig 3D). Consequently, our data showed that CSL3 alleviated the deteriorated ER stress by UVB though autophagy induction.

A)

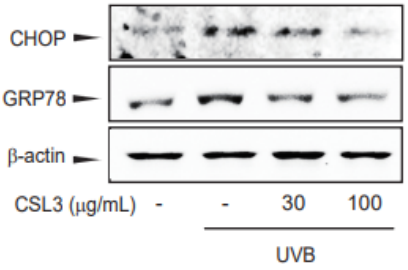

B)

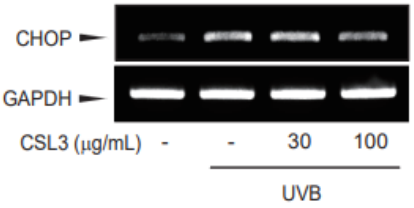

C)

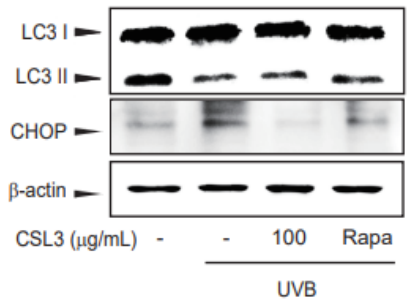

D)

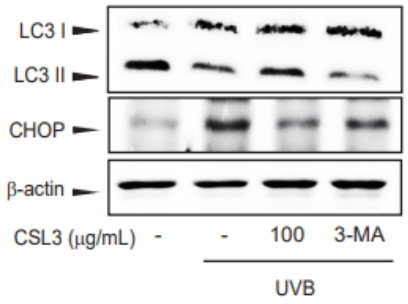

Figure 3. Effects of CSL3 on ER stress in HaCaT cells irradiated with UVB

(A) The property of CSL3 on UVB-induced ER stress. To assess ER stress, HaCaT cells were processed with UVB (30 mJ/cm^2) with or without CSL3 for 3 h. ER stress marker proteins were visualized by immunoblotting. (B) RT-PCR analysis. The effectiveness of CSL3 was confirmed by RT-PCR analysis in the presence or absence of CSL3. HaCaT cells were processed with CSL3 (30 or 100 μg/mL) for 1 h and then processed with UVB (30 mJ/cm^2) for 3 h. (C) HaCaT cells were pretreated with CSL3 (100 μg/mL) or rapamycin (500 nM) for 1 h before treatment with UVB. (D) HaCaT cells were processed with UVB (30 mJ/cm^2) for in the presence of CSL3 (100 μg/mL) for 1 h or 3-MA (50 μM) for 3 h.

4. CSL3 induces autophagy through mTOR pathway

Autophagy is crucial pathway to regulate cell homeostasis [32; 33]. UVB reduced the expression of LC3B-II, representative autophagy induction marker, but CSL3 reversed reduced LC3B-II (Fig 4A). Next, we examined whether CSL3 effect was mediated by mTOR pathway. UVB-induced mTOR phosphorylation was decreased by CSL3 (Fig 4B). Consistently, CSL3 exerted phosphorylation of Akt, a well-known regulator of mTOR activity (Fig 4C). Next, we evaluated MAPK signaling pathway, which is considered as another upstream pathway of mTOR [34]. CSL3 considerably inhibited ERK phosphorylation, but not JNK and p38 (Fig 4D). These results demonstrate that CSL3 has the ability to conserve cells through autophagy induction in UVB-damaged HaCaT cells through mTOR signaling pathway.

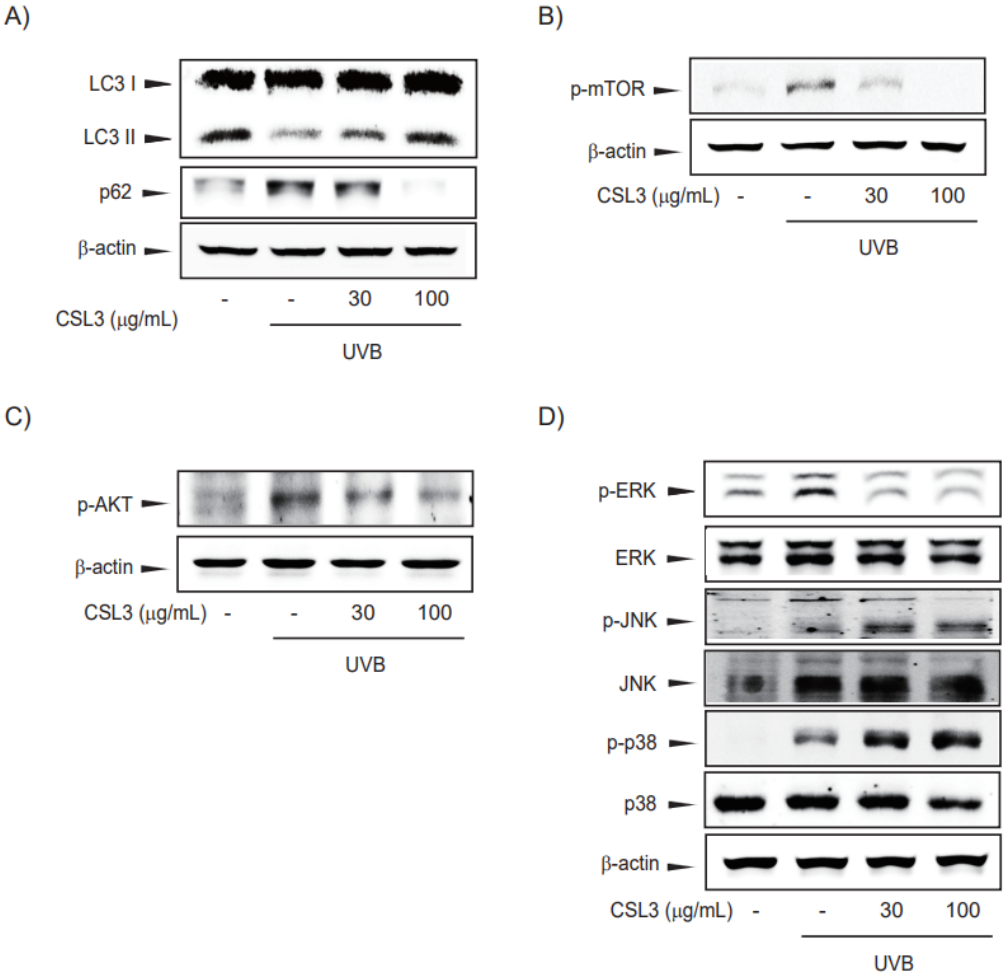

Figure 4. Effects of CSL3 on autophagy in UVB-irradiated HaCaT cells

(A) Effect of CSL3 on autophagy. HaCaT cells were incubated with CSL3 for 1 h and cells were irradiated with UVB (30 mJ/cm^2) for 3 h. LC3B and p62 expression were visualized by immunoblotting. (B, C, D) HaCaT cells were processed with CSL3 for 1 h and cells were then incubated with UVB (30 mJ/cm^2) for 3 h. p-Akt, mTOR, p-mTOR, MAPKs (ERK, p-ERK, JNK, p-JNK, p38, p-p38) were estimated by immunoblotting.

5. CSL3 improves skin aging by UVB

ECM decomposition and increased MMPs are characteristic of skin aging. UVB inhibits collagen synthesis by increasing MMP. We evaluated anti-aging effect of CSL3. Our data showed that UVB prohibited collagen expression, but enhanced MMP-3 and -9 (Fig 5A). AP-1 is organized of c-Jun and c-Fos, and is known to regulate MMP expression [35]. So, we checked phosphorylation level of c-Jun and c-Fos. elevated c-Jun phosphorylation was suppressed by pretreatment of CSL3. However, c-Fos phosphorylation was not affected by CSL3 treatment (Fig 5B). Therefore, we concluded that CSL3 coordinates the expression of MMP through the regulation of c-Jun rather than c-Fos. Next, we identified collagen synthesis and confirmed that UVB definitely decreased collagen synthesis which were inhibited by CSL3 pretreatment (Fig 5C). Furthermore, we evaluated migration of HaCaT by CSL3 through wound healing assay. CSL3 prohibited the decreased migration by UVB irradiation (Fig 5D). The results indicated that CSL3 increase in collagen synthesis in accordance with the decrease MMP expression.

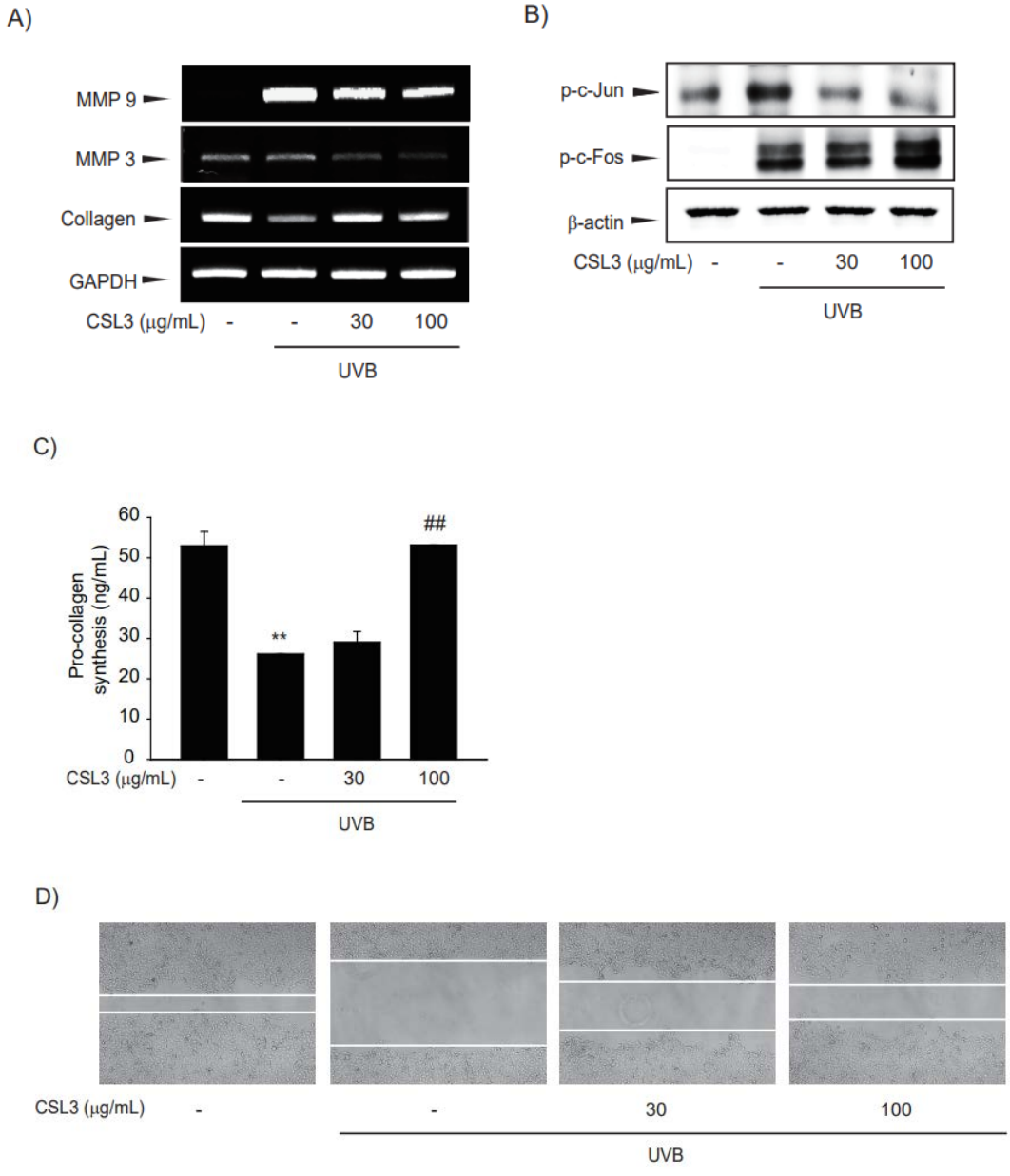

Figure 5. Anti-aging function of CSL3 in HaCaT cells

(A) HaCaT cells were treated with UVB (30 mJ/cm^2) in the presence or absence of CSL3. After 3 h, mRNA levels of collagen and MMP were evaluated by PCR analysis. (B) Cells were processed with CSL3 (30, 100 μg/mL). After 1 h, cells were treated by UVB (30 mJ/cm^2) for 3 h. The protein expression of AP-1 was visualized by immunoblotting. (C) Cells were processed with CSL3 for 1 h and then treated with UVB (30 mJ/cm^2). After 6 h, pro-collagen synthesis was evaluated by using Procollagen Type I C-peptide EIA Kit. (n = 3, significant when compared with controls, **$p<0.01$, compared with the UVB treatment group, ## $p<0.01$) (D) Wound-healing assay. HaCaT cells were cultivated with CSL3 (30 or 100 μg/mL) for 1 h and cells were then incubated with irradiation of UVB (30 mJ/cm^2) for 12 h. The result was visualized by microcopy after UVB treatment.

6. Composition of the CSL extracts and Cytoprotective effect of EGCG in UVB-damaged HaCaT

Next, we analyzed composition of CSL extracts. The overall polyphenol and total flavonoid contents were investigated using colorimetric methods. Gallic acid and quercetin were used as equivalent materials. CSL3 presented the highest content of phenolic compounds. The overall polyphenol and total flavonoid contents of CSL3 were 152.81 ± 7.35 gallic acid equivalent mg/g and 31.72 ± 0.63 quercetin equivalent mg/g, respectively. Similar to the antioxidant activity results, TPC showed that CSL3 was higher than CSL4, indicating that CSL3 contains high-polarity antioxidants. In addition, since flavonoids have relatively low polarity, it was confirmed that TFC was increased during organic solvent extraction (CSL3, CSL4). To identify the components in CSL3 and CSL extracts, we chosen seven phenolic acid and flavonoid standards (gallic acid, epicatechin, epigallocatechin gallate, rutin, tannic acid, naringin, quercetin) and analyzed HPLC. As a result of the experiment, interestingly, the major component of CSL3 was EGCG that is well known the efficient *antioxidant* polyphenol against hydrogen peroxide and radical-scavenging activity [36; 37] (Fig 6A). We evaluated whether CSL3 effect was due to EGCG, major component of CSL3. First, we tested cytotoxic effect of EGCG by using MTT assay. The concentration from 1 μM to 10 μM was not cytotoxic, but the higher concentration showed toxicity (Fig 6B). Thus, we used up to 10 μM of EGCG. EGCG efficiently improved cell viability damaged by UVB-irradiation or *t*-BHP treatment (Fig 6C). We further evaluated whether EGCG could decrease the ROS production caused by UVB. As the result, EGCG reduced intracellular ROS generation induced by UVB and *t*-BHP (Fig 6D). We examined that CSL3 protects UVB-damaged HaCaT through autophagy induction and ER stress inhibition. In line with CSL3, EGCG reversed autophagy reduction by UVB and also decreased ER stress (Fig 6E). Lastly, we investigated the anti-aging function on EGCG. EGCG decreased MMP expression but enhanced collagen expression (Fig 6F). Therefore, our data demonstrated that cytoprotective and anti-aging effect of CSL3 in HaCaT was due to EGCG.

A)

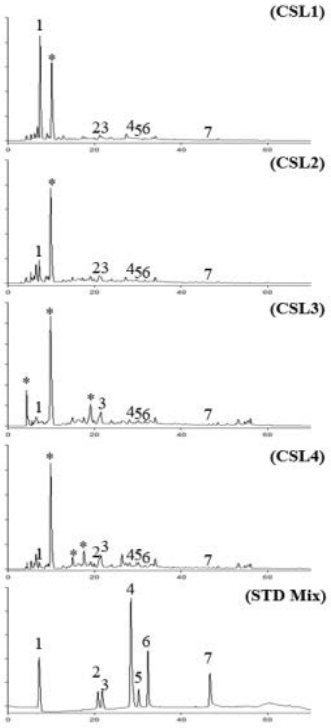

Unit : mg/g

No.	Sample	CSL1	CSL2	CSL3	CSL4
1	Gallic acid	72.98	16.72	1.72	3.05
2	Epicatechin	26.33	22.77	-	16.77
3	Epigallocatechin gallate	10.69	13.18	27.74	12.76
4	Rutin	5.58	5.52	15.56	11.20
5	Tannic acid	5.70	1.33	7.19	6.38
6	Naringin	2.44	-	6.88	3.42
7	Quercetin	1.27	0.67	1.93	1.17

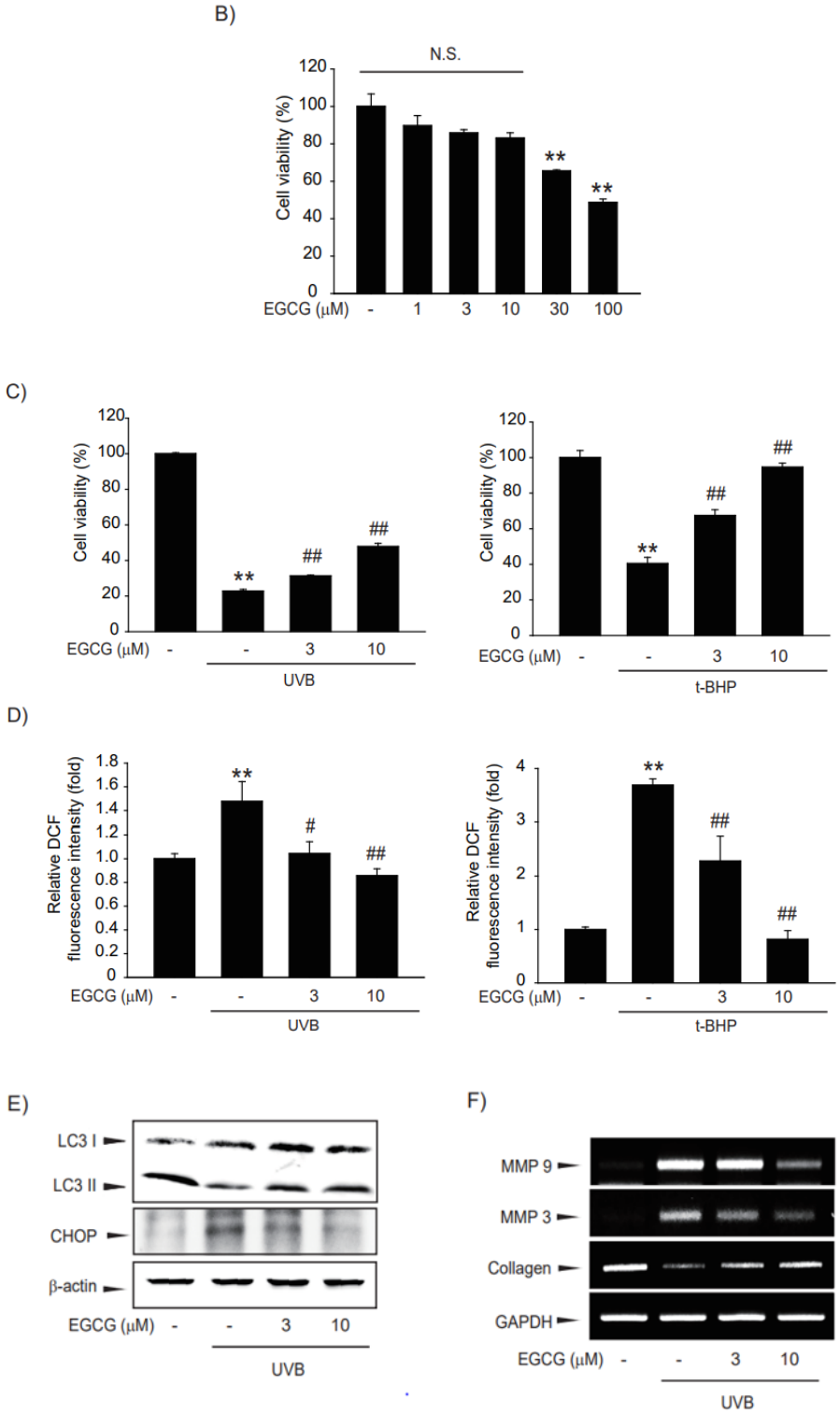

Figure 6. Effects of epigallocatechin (EGCG), the major ingredients of CSL3 on photodamaged by UVB irradiation in HaCaT cells

(A) HPLC chromatogram of CSL extracts. Gallic acid (peak 1), epicatechin (peak 2), EGCG (peak 3), rutin (peak 4), tannic acid (peak 5), naringin (peak 6), quercetin (peak 7). (B) The cytotoxic effect of EGCG in the HaCaT was evaluated at varied concentrations for 12 h by MTT assay. (C) The cytoprotective effect of EGCG on photodamaged HaCaT cells was estimated by MTT assay. The cells were processed with UVB (30 mJ/cm^2) or *t*-BHP (600 μM) in the presence or absence of EGCG for 6 h, and assessed cell viability. (n = 3, significant when compared with controls, **p<0.01, compared with the UVB or *t*-BHP treatment group, ## p<0.01) (D) The effect of EGCG on the intercellular ROS by UVB (30 mJ/cm^2) or *t*-BHP (600 μM) in HaCaT cells. Cells were treated with UVB (30 mJ/cm^2) or *t*-BHP (600 μM) with or without the EGCG. The level of ROS formation was assessed after UVB or *t*-BHP treatment for 1 h (n = 3, significant when compared with controls, **p<0.01, compared with the UVB or *t*-BHP treatment group, # p<0.05, ## p<0.01). (E) HaCaT cells were processed with EGCG for 1 h then treated with UVB (30 mJ/cm^2) for 3 h. Protein expression of autophagy markers (LC3B and p62) and ER stress markers (CHOP, GRP78) were measured by immunoblotting. (F) After pretreatment of CSL3 for 1 h, HaCaT cells were treated with UVB (30 mJ/cm^2) for 3h. RT-PCR analysis was measured 3 h after UVB irradiation.

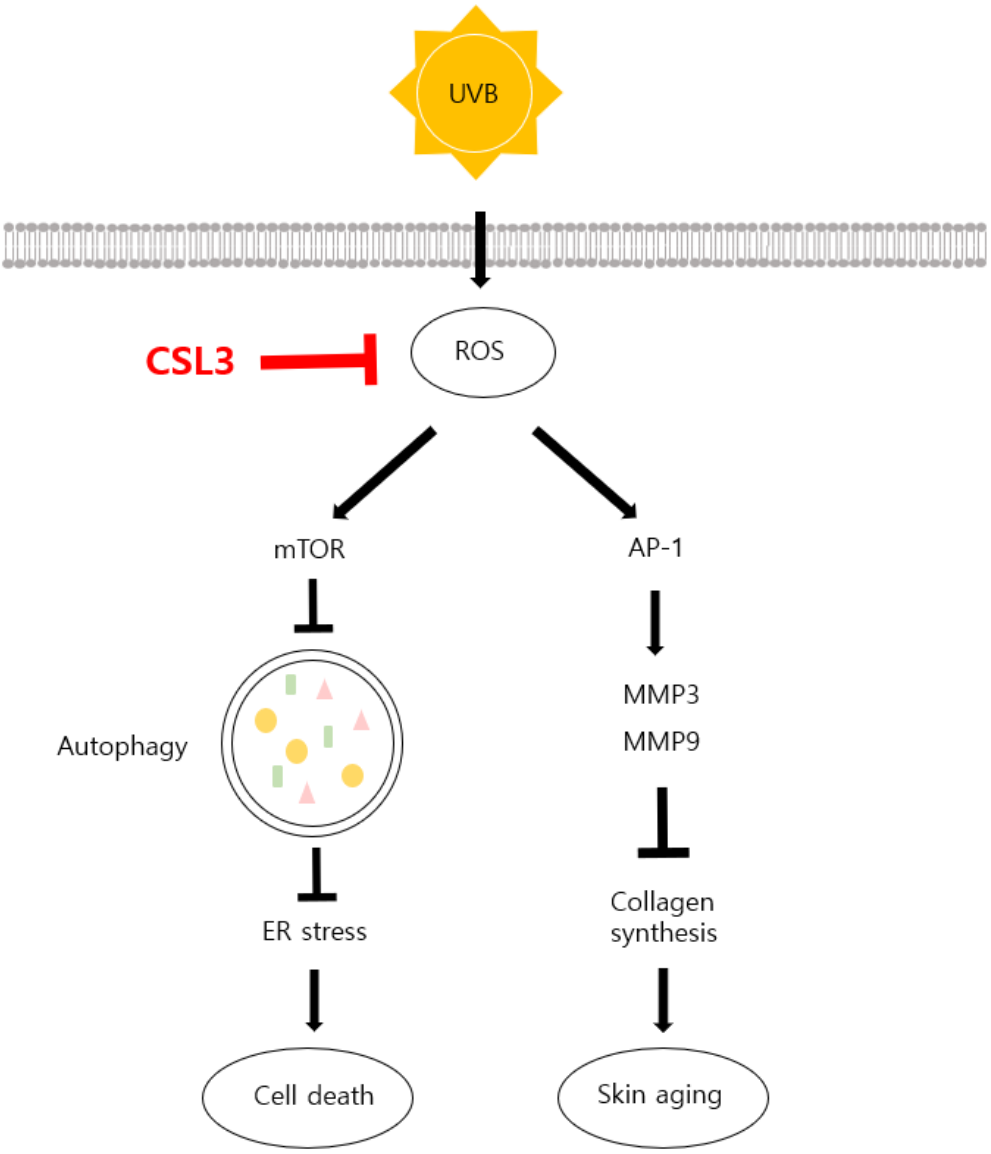

Figure 7. Schematic diagram illustrating the mechanism of CSL3 that protects photodamages and skin aging induced by UVB

IV. DISCUSSION

Protecting skin cells is very crucial because the skin acts as the primary defense organ for our body and is always exposed to external stimuli. In particular, UVB is easily exposed to the external environment and is a major cause of skin diseases [38; 39]. It was well established that UVB increased ROS formation which result in oxidative stress and various damages like to DNA damage and cell death in skin. We found that CSL3 significantly diminished ROS generation induced by UVB or *t*-BHP in HaCaT cells (Fig. 2C). Next, we have examined that the antioxidant efficacy of the CSL3 can protect the HaCaT cell and CSL3 can restore cell viability decreased by UVB irradiation (Fig. 2D). Cell death is roughly divided into programmed and unprogrammed cell death. Apoptosis is a representative example of a programmed cell death and ROS can lead to induce apoptosis [18]. ROS decreases anti-apoptosis factors such as Bcl-2 family but increases apoptosis activator factors such as Bax and PARP-1 [40]. PARP-1 is one of well-known cellular substrates of caspases. Cleavage of PARP-1 by caspases is regarded as a feature of apoptosis [41]. CSL3 reduced the expression of cleaved caspase-3 and PARP-1. In addition, Bax expression was also diminished by the CSL treatment (Fig. 2F). We concluded that the CSL3 reduces ROS formation induced by UVB and protects HaCaT cells through inhibition of apoptosis pathway.

ER stress can arouse skin damage such as skin inflammation, cancer, aging [42; 43] . ER stress is mechanism to protect cells against various stimuli such as UPR, oxidative stress, and UVB irradiation [44]. However, if this ER stress persists, cell death such as apoptosis can be induced. Excessive UPR is staring point of ER stress which activates GRP78, phosphorylates IRE-1, PERK and later activates CHOP [45]. We investigated whether CSL3 can suppress ER stress induced by UVB irradiation. We found that pretreatment of CSL3 inhibited ER stress increased by UVB irradiation (Fig. 3A, B). Our results suggest that CSL3 can reduce skin aging through suppressing ER stress. But, further research is needed to identify molecular

mechanism of CSL3 on ER stress inhibition.

Autophagy is important for maintaining cellular homeostasis by recycling damaged cell organelles [1]. Accumulations of LC3B and reduction of p62 are representative feature of autophagy. Also, mTOR inhibits autophagy by interfering with the formation of autophagosome [46; 47]. Our data showed that CSL3 activated autophagy through mTOR inhibition (Fig. 4B) and activation of p-Akt, a well-known upstream of mTOR (Fig. 4D). We investigated whether ER stress inhibition by CSL3 treatment was through autophagy regulation. 3-Methyladenine, an autophagy inhibitor, increased ER stress markers decreased by UVB irradiation (Fig. 3D) whereas rapamycin, autophagy inducer, reduced ER stress provoked by UVB irradiation (Fig. 3C). Based on the facts that MAPKs are crucial regulators of mTOR and are involved in suppression of ER stress [19], it can be inferred that CSL3-mediated protective effect against UVB irradiation might be reliant on ERK-mTOR signaling. In addition, Akt activity is affected by ERK phosphorylation [48; 49] which may affect UVB-mediated Akt-mTOR pathway. Further studies are still indicated to validate the precise molecular mechanisms of CSL3 effect on UVB irradiation, and these are presently being investigated in our group.

EGCG is found in high content in the green tea and is known to have antioxidant properties [37; 50]. Also, we found that EGCG is major constituents of CSL3 and be higher in content than green tea (Fig. 6A). EGCG is known to have advantageous effect in albumin damaged UVB by preventing ROS [51]. EGCG is known to have advantageous effect in various skin diseases through antioxidant action [52]. Expectedly, our data also indicated that the increased ROS is reduced by EGCG (Fig. 6D). Also, EGCG protected keratinocytes via activation of autophagy and inhibition of ER stress (Fig. 6E). CSL3 has the second most Rutin after EGCG (Fig. 6A). Rutin also has cytoprotective effect in skin fibroblasts damaged by UV by decreasing ROS [53]. Therefore, these results suggest that CSL3 effect on UVB irradiated keratinocyte damage might be due to various polyphenol components including EGCG and Rutin etc.

In conclusion, our data provide that CSL3 can prevent skin aging induced by UVB irradiation through inhibition of MMP and collagen restoration. Also, CSL3 protect the skin by suppressing ER stress through activation of autophagy. Therefore, the results indicate that CSL3 could be a promising candidate against UVB-induced skin photodamage and aging.

V. REFERENCES

[1] Sample, A., and Y. Y. He (2017) Autophagy in UV Damage Response. *Photochem Photobiol*. 93: 943-955.

[2] Park, E. K., H. J. Lee, H. Lee, J. H. Kim, J. Hwang, J. I. Koo, and S. H. Kim (2018) The Anti-Wrinkle Mechanism of Melatonin in UVB Treated HaCaT Keratinocytes and Hairless Mice via Inhibition of ROS and Sonic Hedgehog Mediated Inflammatory Proteins. *Int J Mol Sci*. 19.

[3] Gu, Y., J. Han, C. Jiang, and Y. Zhang (2020) Biomarkers, oxidative stress and autophagy in skin aging. *Ageing Res Rev*. 59: 101036.

[4] Chou, H. Y., D. L. Ma, C. H. Leung, C. C. Chiu, T. C. Hour, and H. D. Wang (2020) Purified Astaxanthin from Haematococcus pluvialis Promotes Tissue Regeneration by Reducing Oxidative Stress and the Secretion of Collagen In Vitro and In Vivo. *Oxid Med Cell Longev*. 2020: 4946902.

[5] Xiao, Z., S. Yang, J. Chen, C. Li, C. Zhou, P. Hong, S. Sun, and Z.-J. Qian (2020) Trehalose against UVB-induced skin photoaging by suppressing MMP expression and enhancing procollagen I synthesis in HaCaT cells. *Journal of Functional Foods*. 74: 104198.

[6] Lin, Z., L. Ni, C. Teng, Z. Zhang, L. Wu, Y. Jin, X. Lu, and Z. Lin (2021) Eicosapentaenoic Acid-Induced Autophagy Attenuates Intervertebral Disc Degeneration by Suppressing Endoplasmic Reticulum Stress, Extracellular Matrix Degradation, and Apoptosis. *Front Cell Dev Biol*. 9: 745621.

[7] Hao, D., X. Wen, L. Liu, L. Wang, X. Zhou, Y. Li, X. Zeng, G. He, and X. Jiang (2019)

Sanshool improves UVB-induced skin photodamage by targeting JAK2/STAT3-dependent autophagy. *Cell Death Dis*. 10: 19.

[8] Song, D., H. Park, S. H. Lee, M. J. Kim, E. J. Kim, and K. M. Lim (2017) PAL-12, a new anti-aging hexa-peptoid, inhibits UVB-induced photoaging in human dermal fibroblasts and 3D reconstructed human full skin model, Keraskin-FT™. *Arch Dermatol Res*. 309: 697-707.

[9] Kwon, K. R., M. B. Alam, J. H. Park, T. H. Kim, and S. H. Lee (2019) Attenuation of UVB-Induced Photo-Aging by Polyphenolic-Rich Spatholobus Suberectus Stem Extract Via Modulation of MAPK/AP-1/MMPs Signaling in Human Keratinocytes. *Nutrients*. 11.

[10] Kim, J. M., S. Y. Kim, E. M. Noh, H. K. Song, G. S. Lee, K. B. Kwon, and Y. R. Lee (2018) Reversine inhibits MMP-1 and MMP-3 expressions by suppressing of ROS/MAPK/AP-1 activation in UV-stimulated human keratinocytes and dermal fibroblasts. *Exp Dermatol*. 27: 298-301.

[11] Jeong, D., N. P. Qomaladewi, J. Lee, S. H. Park, and J. Y. Cho (2020) The Role of Autophagy in Skin Fibroblasts, Keratinocytes, Melanocytes, and Epidermal Stem Cells. *J Invest Dermatol*. 140: 1691-1697.

[12] Karapetsas, A., G. P. Voulgaridou, D. Iliadi, I. Tsochantaridis, P. Michail, S. Kynigopoulos, M. Lambropoulou, M. I. Stavropoulou, K. Stathopoulou, S. Karabournioti, N. Aligiannis, K. Gardikis, A. Galanis, M. I. Panayiotidis, and A. Pappa (2020) Honey Extracts Exhibit Cytoprotective Properties against UVB-Induced Photodamage in Human Experimental Skin Models. *Antioxidants (Basel)*. 9.

[13] Umar, S. A., M. A. Tanveer, L. A. Nazir, G. Divya, R. A. Vishwakarma, and S. A. Tasduq (2019) Glycyrrhizic Acid Prevents Oxidative Stress Mediated DNA Damage

Response through Modulation of Autophagy in Ultraviolet-B-Irradiated Human Primary Dermal Fibroblasts. *Cell Physiol Biochem*. 53: 242-257.

[14] Sano, R., and J. C. Reed (2013) ER stress-induced cell death mechanisms. *Biochim Biophys Acta*. 1833: 3460-3470.

[15] Yin, Y., G. Sun, E. Li, K. Kiselyov, and D. Sun (2017) ER stress and impaired autophagy flux in neuronal degeneration and brain injury. *Ageing Res Rev*. 34: 3-14.

[16] Dossou, A. S., and A. Basu (2019) The Emerging Roles of mTORC1 in Macromanaging Autophagy. *Cancers (Basel)*. 11.

[17] Mlitz, V., G. Gendronneau, I. Berlin, M. Buchberger, L. Eckhart, and E. Tschachler (2016) The Expression of the Endogenous mTORC1 Inhibitor Sestrin 2 Is Induced by UVB and Balanced with the Expression Level of Sestrin 1. *PLoS One*. 11: e0166832.

[18] Piao, M. J., M. J. Ahn, K. A. Kang, Y. S. Ryu, Y. J. Hyun, K. Shilnikova, A. X. Zhen, J. W. Jeong, Y. H. Choi, H. K. Kang, Y. S. Koh, and J. W. Hyun (2018) Particulate matter 2.5 damages skin cells by inducing oxidative stress, subcellular organelle dysfunction, and apoptosis. *Arch Toxicol*. 92: 2077-2091.

[19] Zhang, J., L. Wang, W. Xie, S. Hu, H. Zhou, P. Zhu, and H. Zhu (2020) Melatonin attenuates ER stress and mitochondrial damage in septic cardiomyopathy: A new mechanism involving BAP31 upregulation and MAPK-ERK pathway. *J Cell Physiol*. 235: 2847-2856.

[20] J, K. W., Yoon. E, Yim. S, Park. Y, Kim. G, Song (2011) Antioxidative and Antimicrobial Activities of Castanopsis cuspidata var. sieboldii Extracts. *Korean Journal of Plant Resources*. 24: 200-207.

[21] Y, K. S., M, Song. W, Hyun. S, Yang. C, Song. D, Lee. W, Yoon. (2014) Anti-

inflammatory Effect of Castanopsis cuspidata Extracts in Murine Macrophage RAW 264.7 Cells. *Korean Journal of Plant Resources*. 27: 439-446.

[22] BLOIS, M. S. (1958) Antioxidant Determinations by the Use of a Stable Free Radical. *Nature*. 181: 1199–1200.

[23] Re, R., N. Pellegrini, A. Proteggente, A. Pannala, M. Yang, and C. Rice-Evans (1999) Antioxidant activity applying an improved ABTS radical cation decolorization assay. *Free Radic Biol Med*. 26: 1231-1237.

[24] Ainsworth, E. A., and K. M. Gillespie (2007) Estimation of total phenolic content and other oxidation substrates in plant tissues using Folin-Ciocalteu reagent. *Nat Protoc*. 2: 875-877.

[25] Sawicki, T., M. Starowicz, L. Kłębukowska, and P. Hanus (2022) The Profile of Polyphenolic Compounds, Contents of Total Phenolics and Flavonoids, and Antioxidant and Antimicrobial Properties of Bee Products. *Molecules*. 27.

[26] Yang, J. H., K. M. Kim, M. G. Kim, K. H. Seo, J. Y. Han, S. O. Ka, B. H. Park, S. M. Shin, S. K. Ku, I. J. Cho, and S. H. Ki (2015) Role of sestrin2 in the regulation of proinflammatory signaling in macrophages. *Free Radic Biol Med*. 78: 156-167.

[27] Cieślak, M., J. Kaźmierczak-Barańska, K. Królewska-Golińska, M. Napiórkowska, I. Stukan, U. Wojda, and B. Nawrot (2019) New Thalidomide-Resembling Dicarboximides Target ABC50 Protein and Show Antileukemic and Immunomodulatory Activities. *Biomolecules*. 9.

[28] Youn, U. Y., R. H. Kim, G. N. Kim, and S. C. Lee (2017) Antioxidant and anti-adipogenic activities of the nuts of Castanopsis cuspidata var. thunbergii. *Food Sci Biotechnol*. 26: 1407-1414.

[29] Yin, X., L. Cao, R. Kang, M. Yang, Z. Wang, Y. Peng, Y. Tan, L. Liu, M. Xie, Y. Zhao, K. M. Livesey, and D. Tang (2011) UV irradiation resistance-associated gene suppresses apoptosis by interfering with BAX activation. *EMBO Rep*. 12: 727-734.

[30] Mera, K., K. Kawahara, K. Tada, K. Kawai, T. Hashiguchi, I. Maruyama, and T. Kanekura (2010) ER signaling is activated to protect human HaCaT keratinocytes from ER stress induced by environmental doses of UVB. *Biochem Biophys Res Commun*. 397: 350-354.

[31] Tang, C., M. J. Livingston, Z. Liu, and Z. Dong (2020) Autophagy in kidney homeostasis and disease. *Nat Rev Nephrol*. 16: 489-508.

[32] Chen, X., M. Li, L. Li, S. Xu, D. Huang, M. Ju, J. Huang, K. Chen, and H. Gu (2016) Trehalose, sucrose and raffinose are novel activators of autophagy in human keratinocytes through an mTOR-independent pathway. *Sci Rep*. 6: 28423.

[33] Chun, Y., and J. Kim (2018) Autophagy: An Essential Degradation Program for Cellular Homeostasis and Life. *Cells*. 7.

[34]Yang, Y. H., K. Chen, B. Li, J. W. Chen, X. F. Zheng, Y. R. Wang, S. D. Jiang, and L. S. Jiang (2013) Estradiol inhibits osteoblast apoptosis via promotion of autophagy through the ER-ERK-mTOR pathway. *Apoptosis*. 18: 1363-1375.

[35] Kim, M., Y. G. Park, H. J. Lee, S. J. Lim, and C. W. Nho (2015) Youngiasides A and C Isolated from Youngia denticulatum Inhibit UVB-Induced MMP Expression and Promote Type I Procollagen Production via Repression of MAPK/AP-1/NF-κB and Activation of AMPK/Nrf2 in HaCaT Cells and Human Dermal Fibroblasts. *J Agric Food Chem*. 63: 5428-5438.

[36] Avadhani, K. S., J. Manikkath, M. Tiwari, M. Chandrasekhar, A. Godavarthi, S. M.

Vidya, R. C. Hariharapura, G. Kalthur, N. Udupa, and S. Mutalik (2017) Skin delivery of epigallocatechin-3-gallate (EGCG) and hyaluronic acid loaded nano-transfersomes for antioxidant and anti-aging effects in UV radiation induced skin damage. *Drug Deliv*. 24: 61-74.

[37] Li, D., N. Martini, Z. Wu, S. Chen, J. R. Falconer, M. Locke, Z. Zhang, and J. Wen (2022) Niosomal Nanocarriers for Enhanced Dermal Delivery of Epigallocatechin Gallate for Protection against Oxidative Stress of the Skin. *Pharmaceutics*. 14.

[38] Martinez, R. M., F. A. Pinho-Ribeiro, V. S. Steffen, C. V. Caviglione, J. A. Vignoli, D. S. Barbosa, M. M. Baracat, S. R. Georgetti, W. A. Verri, Jr., and R. Casagrande (2015) Naringenin Inhibits UVB Irradiation-Induced Inflammation and Oxidative Stress in the Skin of Hairless Mice. *J Nat Prod*. 78: 1647-1655.

[39] Sharma, P., M. K. Montes de Oca, A. R. Alkeswani, S. F. McClees, T. Das, C. A. Elmets, and F. Afaq (2018) Tea polyphenols for the prevention of UVB-induced skin cancer. *Photodermatol Photoimmunol Photomed*. 34: 50-59.

[40] Ma, Z. J., L. Lu, J. J. Yang, X. X. Wang, G. Su, Z. L. Wang, G. H. Chen, H. M. Sun, M. Y. Wang, and Y. Yang (2018) Lariciresinol induces apoptosis in HepG2 cells via mitochondrial-mediated apoptosis pathway. *Eur J Pharmacol*. 821: 1-10.

[41] Lin, R. C., S. F. Yang, H. L. Chiou, S. C. Hsieh, S. H. Wen, K. H. Lu, and Y. H. Hsieh (2019) Licochalcone A-Induced Apoptosis Through the Activation of p38MAPK Pathway Mediated Mitochondrial Pathways of Apoptosis in Human Osteosarcoma Cells In Vitro and In Vivo. *Cells*. 8.

[42] Park, K., S. E. Lee, K. O. Shin, and Y. Uchida (2019) Insights into the role of endoplasmic reticulum stress in skin function and associated diseases. *Febs j*. 286: 413-425.

[43] Zhao, M., J. Luo, B. Xiao, H. Tang, F. Song, X. Ding, and G. Yang (2020) Endoplasmic reticulum stress links psoriasis vulgaris with keratinocyte inflammation. *Postepy Dermatol Alergol*. 37: 34-40.

[44] Shu, S., H. Wang, J. Zhu, Z. Liu, D. Yang, W. Wu, J. Cai, A. Chen, C. Tang, and Z. Dong (2021) Reciprocal regulation between ER stress and autophagy in renal tubular fibrosis and apoptosis. *Cell Death Dis*. 12: 1016.

[45] Mao, J., Y. Hu, L. Ruan, Y. Ji, and Z. Lou (2019) Role of endoplasmic reticulum stress in depression (Review). *Mol Med Rep*. 20: 4774-4780.

[46] Hansen, M., D. C. Rubinsztein, and D. W. Walker (2018) Autophagy as a promoter of longevity: insights from model organisms. *Nat Rev Mol Cell Biol*. 19: 579-593.

[47] Chang, N. C. (2020) Autophagy and Stem Cells: Self-Eating for Self-Renewal. *Front Cell Dev Biol*. 8: 138.

[48]Ba, L., J. Gao, Y. Chen, H. Qi, C. Dong, H. Pan, Q. Zhang, P. Shi, C. Song, X. Guan, Y. Cao, and H. Sun (2019) Allicin attenuates pathological cardiac hypertrophy by inhibiting autophagy via activation of PI3K/Akt/mTOR and MAPK/ERK/mTOR signaling pathways. *Phytomedicine*. 58: 152765.

[49] Cao, C., and Y. Wan (2009) Parameters of protection against ultraviolet radiation-induced skin cell damage. *J Cell Physiol*. 220: 277-284.

[50] Wang, L., W. Lee, Y. R. Cui, G. Ahn, and Y. J. Jeon (2019) Protective effect of green tea catechin against urban fine dust particle-induced skin aging by regulation of NF-κB, AP-1, and MAPKs signaling pathways. *Environ Pollut*. 252: 1318-1324.

[51] Szymon, S. M. T. A. V. E. L. U. S. I. B. Z. N. A. S. M. A. R. M. Z. (2018) Epigallocatechin gallate (EGCG) activity against UV light-induced photo damages in

erythrocytes and serum albumin—theoretical and experimental studies. *Journal of Photochemistry and Photobiology A: Chemistry*. 356: 379-388.

[52] Sheng, Y. Y., J. Xiang, J. L. Lu, J. H. Ye, Z. J. Chen, J. W. Zhao, Y. R. Liang, and X. Q. Zheng (2022) Protective effects of gallocatechin gallate against ultraviolet B induced skin damages in hairless mice. *Sci Rep*. 12: 1310.

[53] Gęgotek, A., K. Bielawska, M. Biernacki, I. Dobrzyńska, and E. Skrzydlewska (2017) Time-dependent effect of rutin on skin fibroblasts membrane disruption following UV radiation. *Redox Biol*. 12: 733-744.